CARDIOVASCULAR MEDICINE

Non-invasive evaluation of the myocardial substrate of cardiac amyloidosis by gadolinium cardiac magnetic resonance

E Perugini, C Rapezzi, T Piva, O Leone, L Bacchi-Reggiani, L Riva, F Salvi, L Lovato, A Branzi, R Fattori

Heart 2006;**92**:343–349. doi: 10.1136/hrt.2005.061911

See end of article for authors' affiliations

Correspondence to: Dr Enrica Perugini, Università di Bologna, Istituto di Cardiologia, Ospedale S Orsola-Malpighi, Via Massarenti 9, 40138 Bologna, Italy; e_perugini@hotmail.com

Accepted 27 May 2005
Published Online First 6 June 2005

Objective: To investigate the prevalence and distribution of gadolinium (Gd) enhancement at cardiac magnetic resonance (CMR) imaging in patients with cardiac amyloidosis (CA) and to look for associations with clinical, morphological, and functional features.
Patients and design: 21 patients with definitely diagnosed CA (nine with immunoglobulin light chain amyloidosis and 12 transthyretin related) underwent Gd-CMR.
Results: Gd enhancement was detected in 16 of 21 (76%) patients. Sixty six of 357 (18%) segments were enhanced, more often at the mid ventricular level. Transmural extension of enhancement within each patient significantly correlated with left ventricular (LV) end systolic volume ($r = 0.58$). The number of enhanced segments correlated with LV end diastolic volume ($r = 0.76$), end systolic volume ($r = 0.6$), and left atrial size ($r = 0.56$). Segments with $> 50\%$ extensive transmural enhancement more often were severely hypokinetic or akinetic ($p = 0.001$). Patients with > 2 enhanced segments had significantly lower 12 lead QRS voltage and Sokolow-Lyon index. No relation was apparent with any other clinical, morphological, functional, or histological characteristics.
Conclusion: Gd enhancement is common but not universally present in CA, probably due to expansion of infiltrated interstitium. The segmental and transmural distribution of the enhancement is highly variable, and mid-ventricular regions are more often involved. Enhancement appears to be associated with impaired segmental and global contractility and a larger atrium.

Amyloidosis is a rare disease characterised by extracellular accumulation of fibrillary proteins, leading to loss of normal tissue architecture. Cardiac involvement—in the form of cardiac amyloidosis (CA)—is rather common and is an adverse prognostic marker.[1] On cardiological grounds, the two most clinically relevant types of amyloidosis are: (1) acquired monoclonal immunoglobulin light chain amyloidosis, characterised by clonal plasma cells in the bone marrow, which produce the immunoglobulin lights chains of the fibrillary deposit; and (2) the hereditary, transthyretin related form of amyloidosis, which is caused by mutant transthyretin, a transport protein mainly synthesised by the liver.

Gadolinium cardiac magnetic resonance (Gd-CMR) imaging has been used for non-invasive evaluation of the myocardial substrate in ischaemic, dilated, and hypertrophic cardiomyopathies,[2–7] myocarditis,[8] and storage diseases.[9 10] As an extracellular fluid tracer, Gd accumulates in expanded interstitial space without crossing intact cell membranes.

We previously reported on the use of conventional CMR in the diagnosis of CA.[11] Gd-CMR may provide relevant additional information to help understand CA on pathophysiological and morphological grounds, since the amyloid deposits induce major interstitial expansion. To this end, we investigated the prevalence and distribution of Gd-CMR enhancement in patients with CA and looked for associations with clinical, morphological, and functional features.

METHODS

Eligibility criteria

All patients with a definite diagnosis of CA under observation in our institute between December 2002 and January 2004 were prospectively studied with Gd-CMR. Inclusion criteria for the study were histologically proven systemic amyloidosis and echocardiographic diagnosis of cardiac involvement. Cardiac involvement was defined as end diastolic thickness of the interventricular septum > 1.2 cm (in the absence of any other cause of ventricular hypertrophy) plus two or more of the following echocardiographic findings: (1) homogeneous atrioventricular valve thickening; (2) atrial septal thickening; and (3) sparkling appearance of the ventricular septum.[12] Exclusion criteria were evidence of atherosclerotic coronary artery disease, based either on coronary arteriography or on pathological inspection of hearts (after transplantation or death) and a history of myocardial infarction. All patients received complete clinical assessment, 12 lead ECG echocardiography, and Gd-CMR. All patients provided prior written informed consent for this Gd-MRI study and for anonymous publication of data. The study was planned and performed in line with the principles of the Declaration of Helsinki.

Echocardiography

Echocardiograms were obtained by a Hewlett Packard Sonos 5500 echocardiograph with a multifrequency phased array probe. Bidimensional and Doppler technique were used. M mode measures were obtained according to the recommendations of the American Society of Echocardiography.[13] Early (E wave) and late (A wave) peak left ventricular (LV) filling velocities, E:A ratio, and E wave deceleration time were measured from the transmitral pulsed Doppler velocity

Abbreviations: CA, cardiac amyloidosis; CMR, cardiac magnetic resonance; FIESTA, fast imaging employing steady state acquisition; Gd, gadolinium; LV, left ventricular

recordings, with the sample volume positioned at the tips of the mitral valve leaflets. Restriction was diagnosed when the following criteria were satisfied: deceleration time < 150 ms; and E to A wave velocity ratio > 2.5.[14]

Electrocardiogram

ECGs were obtained and analysed for standard characteristics and for total 12 lead QRS voltage, defined as the sum of the amplitude of QRS complexes from the peak of the R wave to the maximum dip of the S or Q wave, whichever was greatest, in precordial and limb leads.[15]

Gd-CMR protocol

CMR images were acquired with a 1.5 T scanner (Signa Horizon, GE Medical Systems, Milwaukee, Wisconsin, USA) equipped with a cardiac phased array coil. Coronal, transaxial, and two chamber views were obtained as scout images. Breath hold cine magnetic resonance sequence with steady state free precession by fast imaging employing steady state acquisition (FIESTA) (GE Medical Systems) was performed, covering the whole LV in the short axis plane from apex to atrioventricular ring, and in four chamber view. The sequence parameters were as follows: repetition time, 4 ms; echo time, 1.7 ms; flip angle, 45°; matrix, 256 × 192; field of view, 320 mm; section thickness, 7 mm without spacing; and NEX 1. Gadopentate dimeglumine (Magnevist; Schering, Berlin, Germany) (0.2 mmol/kg) was administered intravenously at 4 ml/s.

After a 10–15 minute delay, a segmented inversion recovery fast gradient echo sequence was performed in the short axis plane of the LV and in four chamber view—identical to those used for FIESTA—with slice thickness of 7 mm and gap of 0 mm. Repetition time of 5.3 ms, echo time of 1.3 ms, flip angle of 20°, matrix of 256 × 160, NEX 2, and field of view of 320 mm were used. Optimal inversion times to null the normal myocardial signal were determined for each patient (230–400 ms, median 280).

Gd-CMR image analysis

Cine CMR images were evaluated by using an image analysis workstation (Advanced Windows 4.0; GE Medical Systems). Ventricular volumes, LV ejection fraction, parietal thicknesses and mass, interatrial septal thickness, and left atrial diameter were measured by tracing epicardial or endocardial borders manually with commercially available software (Mass Analysis Plus; Medis, Leiden, the Netherlands). The 17 segment model recommended by the American Heart Association was used to assess regional thickness, kinesis, and Gd enhancement of the LV.[16] Segmental wall motion was visually assessed (kinetics score) as normal (score of 0), moderate hypokinesis (1), severe hypokinesis (2), akinesis (3), and dyskinesis (4). The transmural extent of hyperenhanced tissue within each segment was scored (Gd enhancement score) visually on a five point scale as < 1% (no enhancement, score of 0), 1–25% (of the total thickness enhanced, score of 1), 26–50% (score of 2), 51–75% (score of 3), and 76–100% (score of 4).[2 3] Additionally, to provide semiquantitative characterisation of both the perimetric and transmural extent of Gd enhancement, a global enhancement severity score was created: this was defined as the sum of the individual enhancement scores of all enhanced segments in each patient. Assessment of the right ventricle focused on maximum diastolic thickness of the wall and presence of Gd enhancement at this level.

Myocardial biopsies

All available myocardial biopsy samples were fixed by microwave irradiation for five minutes in 10% buffered formalin, processed in a microwave oven, and embedded in paraffin. Multiple sections were histologically examined by standard haematoxylin and eosin, Mallory trichrome, and Congo red stains to identify the presence of amyloid by green birefringence under polarised light.

The following variables were considered for assessment of amyloid deposits: location (endocardial, interstitial, and vascular), type of distribution (multifocal, diffuse), and pattern of deposition in myocardial interstitium (interstitial perimyocitic, interstitial nodular, or mixed). The amount of amyloid deposits was classified according to the following semiquantitative method: mild (< 30% involvement of the tissue fragments); moderate (30–60%); and severe (> 60% involvement).[17] The entity of myocardial damage was classified as follows: mild (if myocytes showed hypertrophy, mild atrophy, and mild sarcoplasmic vacuolisation); moderate (thin myocytes compressed into focal areas and showing intense sarcoplasmic vacuolisation); and severe (widespread thin, compressed, and fragmented myocytes).

Statistical analysis

Data were statistically analysed by SPSS 11.0 statistical software (SPSS Inc, Chicago, Illinois, USA). Continuous variables were expressed as the mean (SD) (or median and range, when specified); categorical variables were expressed as percentages. On the basis of available numbers, subgroups were compared by non-parametric tests (Mann-Whitney U or Kruskal-Wallis) or contingency tables, as appropriate. Spearman's correlation coefficient was calculated to assess correlation between variables and linear regression was analysed. Values of $p < 0.05$ were considered significant.

RESULTS

Patient population

Twenty one patients satisfied the eligibility criteria. All patients completed the study protocol. Nine patients had immunoglobulin light chain amyloidosis. Twelve had transthyretin related amyloidosis, nine carrying either the Gln89 transthyretin mutation (n = 3), Lys54 (n = 1), Pro36 (n = 1), Ala49 (n = 2), or Leu68 (n = 2), and three having ''senile'' wild-type transthyretin related amyloidosis. Table 1 summarises relevant clinical, morphological, and functional findings at the time of the study.

Prevalence and distribution of Gd enhancement

Figure 1 shows a representative example of Gd enhancement (accompanied by images obtained by conventional CMR and by subsequent histopathological examination). Gd enhancement

Table 1 Clinical, morphological, and functional variables in the overall patient population (n = 21)

Age (years)	61 (14)
Men:women	13:8
Monoclonal immunoglobulin light chain amyloidosis	9 (43%)
Transthyretin related amyloidosis	12 (57%)
Atrial fibrillation	5 (24%)
New York Heart Association class	
I/II	14 (66%)
III	7 (34%)
Cardiac magnetic resonance parameters	
IVS thickness (mm)	16 (4)
LV mass (g/m^2)	188 (786)
LV diastolic volume (ml/m^2)	68 (14)
LV systolic volume (ml/m^2)	34 (9)
LV ejection fraction (%)	50 (9)
LA diameter (mm)	47 (7)
Echocardiographic indices of LV filling	
Deceleration time (ms)	182 (290
Restrictive filling pattern	7 (33%)

Data are mean (SD) or number (%).
IVS, interventricular septum; LA, left atrium; LV, left ventricular.

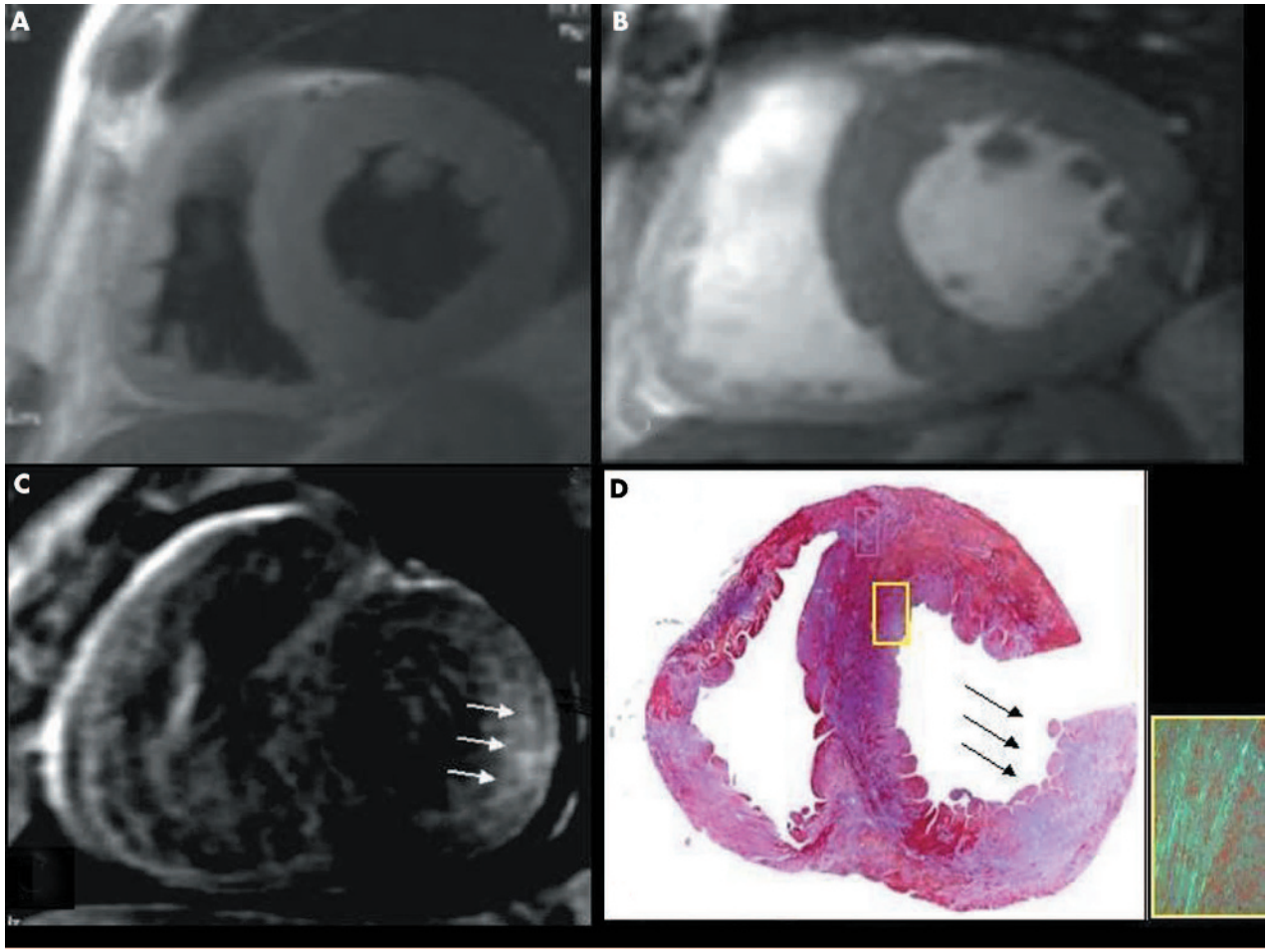

Figure 1 In a 43 year old man with familial transthyretin related cardiac amyloidosis, conventional cardiac magnetic resonance (CMR) with (A) black blood fast spin echo and (B) bright blood fast gradient echo sequences shows increased left and right ventricular thicknesses. (C) Gadolinium (Gd) CMR inversion recovery fast gradient echo also shows a large transmural zone of strong, patchy hyperenhancement (arrows). (D) After combined heart and liver transplantation, myocardial histological analysis showed diffuse amyloid deposition with characteristic green birefringence on Congo red staining (inset) and an area of massive infiltration (arrows) corresponding to the strong, patchy enhancement seen on Gd-CMR.

was found in 16 of 21 patients, corresponding to a prevalence of 76%. Among the 357 LV and septal segments analysed in the total population, 66 (18%) displayed Gd enhancement. Each patient had a median of two (range 0–10, mean 3.0 (2.7)) enhanced segments. The transmural distribution of the Gd enhancement score varied among the 66 enhanced segments.[2 3] The score was 1 in 13 segments (20%), 2 in 16 (24%), 3 in four (6%), and 4 in 33 (50%).

In the 17 segment model,[16] high enhancement scores (defined as 3 or 4) were more often recorded at the mid ventricular level (25 of 126 (20%)) than in the basal (11 of 126 (9%)) and apical (seven of 105 (7%)) levels ($p = 0.003$).

Figure 2 shows representative examples of the two main enhancement patterns (localised and diffuse) that we observed. Among the 16 patients with Gd enhancement, the pattern was localised in 12 and diffuse in four.

As regards the right ventricle, zones of subendocardial Gd enhancement were observable in three patients (all of whom also had LV involvement).

Influence of Gd enhancement on segmental contractility

Among the 357 segments, the kinetics score was 0–1 in 278 (78%) and 2–3 in 79 (22%); none of the segments was dyskinetic. The presence of Gd enhancement appeared to influence segmental dysfunction: kinetics scores > 1 were found in only 19% (61 of 320) of segments with low enhancement scores (0–2) compared with 46% (17 of 37) with high enhancement scores (> 2) ($p = 0.001$) (fig 3).

Clinical, morphological, and functional variables and Gd enhancement

Comparing patients with and without Gd enhancement, no significant difference was apparent in terms of age, New York Heart Association class, or aetiology (of note, the number of enhanced segments in patients with the senile form was 0.6 (0.5) compared with 3.6 (2.0) for immunoglobulin light chain amyloidosis and 3.8 (3.0) for the hereditary transthyretin related form; $p = 0.21$).

In subgroup analysis based on the median number of enhanced segments ($\leqslant 2$ *v* > 2), the variables that differed significantly between the two subgroups were total 12 lead QRS amplitude (117 (48) mV *v* 83.6 (24) mV, $p = 0.047$) and Sokolow-Lyon index (21 (10) mV *v* 13 (3.5) mV, $p = 0.018$), which were both lower among patients with > 2 enhanced segments. We also looked for evidence of a correlation between Gd enhancement and clinical, morphological, and functional variables among patients with at least one enhanced segment, considering the number of enhanced segments and global enhancement severity score as independent variables. On CMR, the global enhancement severity score correlated with LV systolic volume ($r = 0.58$,

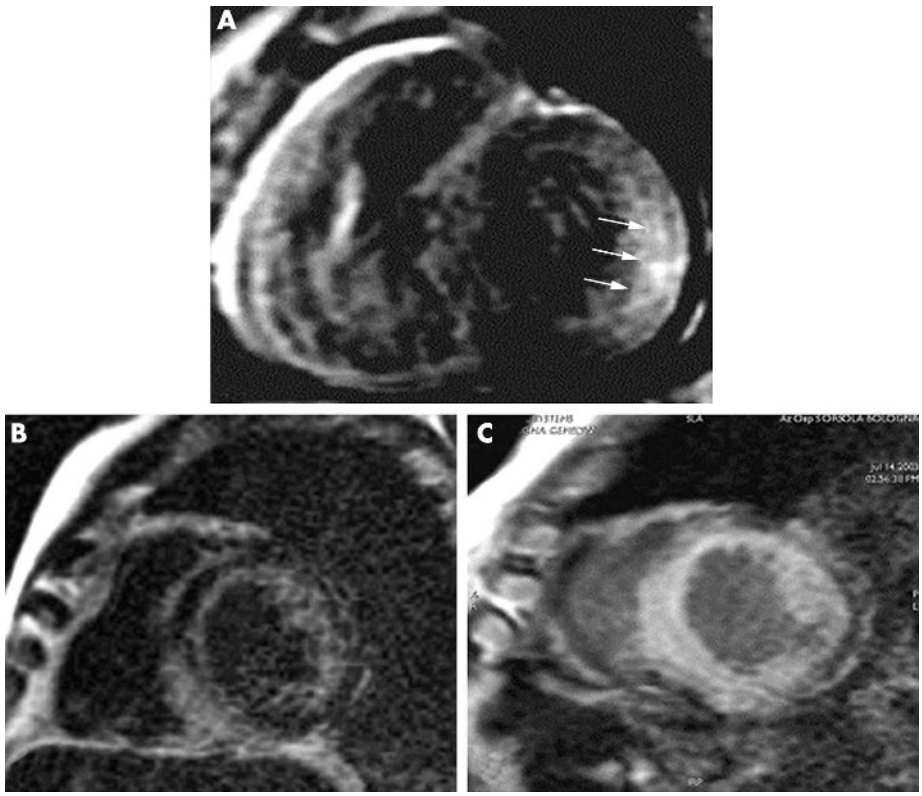

Figure 2 Post-contrast Gd-CMR images (segmented inversion recovery fast gradient echo sequences in short axis view) showing representative examples of the main enhancement patterns. (A) Localised enhancement, mainly in the posterolateral mid ventricular segment (arrows); note that the non-enhanced myocardium is nulled by the inversion recovery pulse. (B) Diffuse subendocardial enhancement (particularly evident at the posterolateral level). (C) Diffuse, intense transmural enhancement observable throughout the entire ventricular section.

p = 0.018) (fig 4) and number of enhanced segments correlated with the following parameters: end systolic left atrium diameter (r = 0.56, p = 0.024) (fig 4), LV end diastolic volume (r = 0.764, p = 0.001), and end systolic volume (r = 0.607, p = 0.021).

Histological features and DE

Right ventricle endomyocardial biopsies were available from 15 patients (4–6 endomyocardial tissue samples were obtained from each in the standard fashion from the right side of the interventricular septum). Table 2 shows the principal findings. Notably, in all patients both the amount of amyloid and the global myocardial damage were always moderate or severe. Amyloid had infiltrated the interstitium

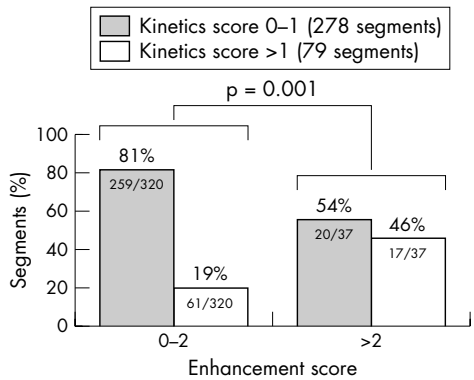

Figure 3 Association between Gd enhancement (score $\leqslant 2$ v >2) and segmental dysfunction (kinetics score $\leqslant 1$ v >1) among the 306 myocardial segments analysed. Segments with more extensive transmural enhancement had a higher prevalence of severe hypokinesia or akinesia.

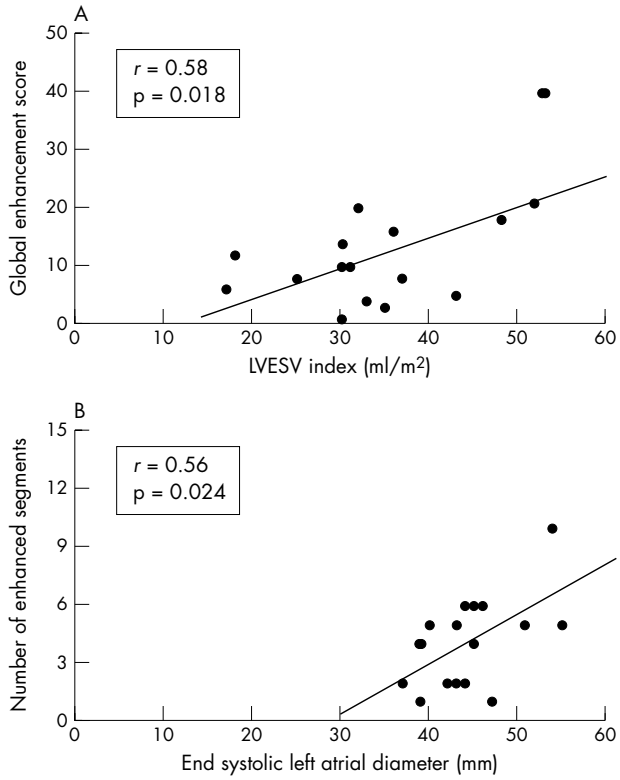

Figure 4 Linear regression analysis of the correlation between left ventricular end systolic volume (LVESV) at CMR and global enhancement severity score (panel A), and between end systolic left atrial diameter and numbers of Gd enhanced segments (panel B).

Table 2 Histological features of 15 patients with myocardial biopsy according to the presence of gadolinium enhancement

		Myocardial enhancement		
	All patients (n = 15)	Present (n = 12)	Absent (n = 3)	p Value*
Amount of amyloid deposit				
Moderate	10 (66%)	7 (58%)	3 (100%)	0.49
Severe	5 (34%)	5 (42%)	0 (0%)	0.49
Location				
Endocardial	11 (73%)	9 (75%)	3 (100%)	0.87
Interstitial	15 (100%)	12 (100%)	3 (100%)	1
Vascular	7 (47%)	5 (42%)	2 (66%)	0.89
Global myocardial damage				
Mild	0 (0%)	0 (0%)	0 (0%)	1
Moderate	11 (73%)	9 (75%)	2 (67%)	0.66
Severe	4 (27%)	3 (25%)	1 (33%)	0.66

*Enhancement versus no enhancement.

in all 15 (100%) patients, the subendocardial layer in 11 (73%), and intramural coronary vessel walls in seven (47%). Inflammatory infiltrate was evident in two (13%) patients. No significant histological difference was observable between patients with and without Gd enhancement.

DISCUSSION

This study of Gd enhancement on Gd-CMR extends our knowledge of myocardial involvement in systemic amyloidosis, showing a relation between the myocardial substrate and ventricular function.

In our clearly defined population of patients with immunoglobulin light chain or transthyretin related amyloidosis bearing a consolidated echocardiographic diagnosis of CA, we found a remarkably high prevalence of Gd enhancement (in about three quarters of our patients) and an association with LV segmental dysfunction. This finding requires explanation in the light of our knowledge of the general rules of Gd accumulation and of the specific histology of CA. Gd is an inert extracellular agent that cannot cross intact sarcolemmal membranes. In the normal myocardium, where the tissue volume is predominantly intracellular, the distribution volume of Gd is normally very low and Gd enhancement is absent. When interstitial space expands, Gd concentration increases within myocardial tissue.[18 19] In CA, the interstitium is expanded due to extracellular amyloid infiltration. Thus, interstitial Gd accumulation due to amyloid infiltration is a highly plausible explanation for the very high prevalence of Gd enhancement. Nevertheless, several other possible contributory causes must also be considered. For instance, Gd has been shown to accumulate diffusely after acute myocarditis due to interstitial expansion caused by the inflammatory infiltrate (a major inflammatory infiltrate was present in two of our 15 patients with available myocardial biopsy, both of whom had Gd enhancement). Furthermore, we cannot completely exclude the possibility that amyloid surrounding the myocytes may damage the cellular membranes, allowing Gd to penetrate the intracellular space. Lastly, since amyloid is often deposited in intramural arteries, leading to ischaemia in the context of normal epicardial vessels,[20] Gd may also accumulate in necrotic scars. However, the possibility that interstitial or post-necrotic fibrosis can provide a myocardial substrate for Gd accumulation seems unlikely, since it was absent in each of the 15 patients for whom a myocardial biopsy was available.

Widespread interstitial accumulation of amyloid can also explain the diffuse pattern of Gd enhancement observed in a minority of our patients. Although uncommon, this pattern appears quite distinctive with respect to previous descriptions of other myocardial abnormalities. For instance, patients with dilated cardiomyopathy and normal coronary arteries with Gd enhancement can display either a focal subendocardial transmural pattern indistinguishable from that of ischaemic patients or a longitudinal patchy mid wall enhancement outside the territory of a coronary artery, probably reflecting myocardial fibrosis.[5] In hypertrophic cardiomyopathy Gd enhancement is common (with focal or diffuse patterns).[6 7] Gd enhancement has also recently been reported in two storage myocardial diseases, namely glycogenosis[9] and Anderson-Fabry disease.[10] In Anderson-Fabry disease the accumulation was mainly localised to the basal inferolateral LV wall and was not subendocardial (interstitial fibrosis has been hypothesised as the substrate).

It remains to be explained why Gd enhancement was absent in about 80% of the ventricular segments and was completely undetectable in five (24%) patients, all of whom had a definite echocardiographic and histological diagnosis of CA. These observations are somewhat surprising in a disease that is characterised by widespread myocardial infiltration by amyloid. We can only speculate that a widespread, uniform myocardial infiltration of amyloid could have precluded the localised differences in signal intensity, which is a prerequisite for the recognition of areas of Gd enhancement.

In the one other available study on Gd enhancement in CA, Maceira *et al*[21] analysed a series of patients with CA alongside a comparison group characterised by hypertensive cardiomyopathy. Although 69% of the patients in the CA group had late hyperenhancement, the phenomenon tended to be global and subendocardial. The discrepancy with the limited number of enhanced segments recorded from our patients may be explained by at least four considerations: firstly, technical or procedural differences could have led to different levels of sensitivity; secondly, our population contained a higher proportion of patients with aetiology other than monoclonal immunoglobulin light chain amyloidosis (hereditary transthyretin related and senile type); thirdly, our patients had less severe cardiomyopathies (restrictive physiopathology was not a diagnostic inclusion criterion); and lastly, more generally, the histopathological profile of cardiac amyloidosis appears to be highly heterogeneous, with variable impairment of the subendocardial and subepicardial layers and preservation of central portions of the myocardium in the context of different histological patterns (nodular, reticular, etc).[17 22 23]

As regards image quality, we very often encountered suboptimal images with a low signal to noise ratio, a phenomenon that has been previously reported in the context of amyloid infiltration of both myocardium and soft tissues.[11 24 25] The mechanism underlying this characteristic low signal to noise ratio remains uncertain: loss of signal may depend on the compact and complex environment of the

amyloid extracellular matrix or magnetic field non-uniformity due to decreased proton density.[24 25]

An additional objective of the study was to look for factors possibly related to Gd enhancement. A comparison between patients with and without Gd enhancement did not show any difference in the distribution of clinical, morphological, and functional variables, perhaps because of the limited number of patients. We extended the search for relations between Gd enhancement and patient related variables by assessing the extent of Gd enhancement. Since the enhancement pattern was not dense or scar-like, a perimetric evaluation did not seem appropriate. We therefore adopted a semiquantitative approach based on the number of involved segments and the transmural extension within each segment, scored from 0 to 4. In addition, we devised a global enhancement severity score for each patient by summing the enhancement scores of the various enhanced segments. The number of segments involved was very variable (maximum 10, median 2); the mid ventricular segments were those most affected.

Patients with more than two enhanced segments had lower QRS voltage on the ECG, with significantly lower total 12 lead QRS amplitude and Sokolow-Lyon index. This observation fits the interpretation that the Gd enhancement was predominantly due to interstitial amyloid infiltration—itself the classic explanation for ECG abnormalities in CA.

An interesting association was recorded between the amount of transmural enhancement and segmental dysfunction: patients with more extensive transmural enhancement had a higher prevalence of severe hypokinesia or akinesia (fig 3). Since amyloid deposition is extracellular, it should not interfere with the myocardial cells' intrinsic contractile function. However, when deposition becomes widespread, the amyloid surrounding the myocardial cells can provoke functional isolation, thus interfering with the development of adequate systolic tension during ejection. The role of myocardial ischaemia caused by amyloid infiltration of small arteries, a characteristic feature of CA, may also be important.

Among the 14 patients with enhancement, the global enhancement severity score correlated with LV end systolic volume (fig 4). This finding suggests that Gd enhancement may be related to reduced contractility both at the segmental and at the global LV levels. As for LV diastolic function, no correlation was observable between Gd enhancement and echocardiographic Doppler indices of LV filling. Nevertheless, left atrial size—a reflection of both systolic and diastolic LV function—did correlate with the number of enhanced segments. Lack of an apparent correlation between LV mass and any index of enhancement extension may be explained by the small number of patients or their particularly high average LV mass.

A specific feature of the study was the availability of histological information for over half the population. The absence of observed relations between Gd enhancement and histological features may seem puzzling, since Gd-CMR explores the interstitium, which can also be investigated by histological analysis. However, biopsy specimens are derived from casual sampling of the right side of the interventricular septum and thus may not be representative of the overall myocardial infiltration. Furthermore, the presence of moderate to severe myocardial amyloid infiltration in all 15 patients could have hampered the recognition of interindividual variations in Gd enhancement.

Study limitations

It must be stressed that this mainly descriptive study did not have a diagnostic or strictly clinical goal. Instead, it was conceived to gain knowledge regarding the potential of Gd enhancement as a non-invasive descriptor of the myocardial substrate in CA. Analysis was limited by numbers, due to the rarity of amyloidosis. This factor might have impeded recognition of differences in clinical, morphological, and instrumental factors between the two subgroups. On technical grounds, it should be noted that the decision to focus on zones and patterns of Gd enhancement rather than on Gd kinetics could have led to an underestimate of the phenomenon (and indirectly also to suboptimal image quality). Similar considerations can be made regarding the image acquisition times (after a 10–15 minute delay, in line with standard procedures) in our Gd-CMR protocol: use of a much shorter delay (as innovatively used by Maceira *et al*[21]) might have led to improved enhancement detection. As regards the right ventricle (where three of our patients had observable enhancement), it must be pointed out that for technical and anatomical reasons assessment of Gd enhancement is very difficult in this site.

Conclusions

Myocardial Gd enhancement appears to be a very common—albeit not universal—feature in both the transthyretin related and immunoglobulin light chain forms of CA. The enhancement is probably largely due to variable expansion of infiltrated interstitium. Segmental and transmural distribution of the Gd enhancement appears to be highly variable, with the mid ventricular regions being more often involved. Moreover, Gd enhancement appears to be associated with impaired segmental and global contractility and a larger atrium. Gd-CMR provides a unique opportunity for non-invasive study of amyloid myocardial infiltration and its pathophysiological consequences. Further studies should explore the clinical utility of Gd-CMR in CA, including the potential prognostic implications of these observations.

ACKNOWLEDGEMENTS

We are grateful to Robin M T Cooke for writing assistance.

Authors' affiliations

E Perugini, C Rapezzi, L Bacchi-Reggiani, L Riva, A Branzi, Institute of Cardiology, University of Bologna, S: Orsola-Malpighi Hospital, Bologna, Italy
T Piva, L Lovato, R Fattori, Department of Radiology, University of Bologna, S: Orsola-Malpighi Hospital
O Leone, Department of Pathology, University of Bologna, S: Orsola-Malpighi Hospital
F Salvi, Department of Neurology, Ospedale Bellaria, Bologna, Italy

We declare no competing interests.

REFERENCES

1 **Falk RH**, Comenzo RL, Skinner M. The systemic amyloidoses. *N Engl J Med* 1997;**337**:898–909.
2 **Wu E**, Judd RM, Vargas JD, *et al*. Visualisation of presence, location, and transmural extent of healed Q-wave and non-Q-wave myocardial infarction. *Lancet* 2001;**357**:21–8.
3 **Kim RJ**, Wu E, Rafael A, *et al*. The use of contrast-enhanced magnetic resonance imaging to identify reversible myocardial dysfunction. *N Engl J Med* 2000;**343**:1445–53.
4 **Beek AM**, Kuhl HP, Bondarenko O, *et al*. Delayed contrast-enhanced magnetic resonance imaging for the prediction of regional functional improvement after acute myocardial infarction. *J Am Coll Cardiol* 2003;**42**:895–901.
5 **McCrohon JA**, Moon JC, Prasad SK, *et al*. Differentiation of heart failure related to dilated cardiomyopathy and coronary artery disease using gadolinium-enhanced cardiovascular magnetic resonance. *Circulation* 2003;**108**:54–9.
6 **Moon JC**, McKenna WJ, McCrohon JA, *et al*. Toward clinical risk assessment in hypertrophic cardiomyopathy with gadolinium cardiovascular magnetic resonance. *J Am Coll Cardiol* 2003;**41**:1561–7.
7 **Choudhury L**, Mahrholdt H, Wagner A, *et al*. Myocardial scarring in asymptomatic or mildly symptomatic patients with hypertrophic cardiomyopathy. *J Am Coll Cardiol* 2002;**40**:2156–64.
8 **Friedrich MG**, Strohm O, Schulz-Menger J, *et al*. Contrast media-enhanced magnetic resonance imaging visualizes myocardial changes in the course of viral myocarditis. *Circulation* 1998;**97**:1802–9.
9 **Moon JC**, Mundy HR, Lee PJ, *et al*. Images in cardiovascular medicine. Myocardial fibrosis in glycogen storage disease type III. *Circulation* 2003;**107**:e47.

10 **Moon JC**, Sachdev B, Elkington AG, *et al*. Gadolinium enhanced cardiovascular magnetic resonance in Anderson-Fabry disease: evidence for a disease specific abnormality of the myocardial interstitium. *Eur Heart J* 2003;**24**:2151–5.
11 **Fattori R**, Rocchi G, Celletti F, *et al*. Contribution of magnetic resonance imaging in the differential diagnosis of cardiac amyloidosis and symmetric hypertrophic cardiomyopathy. *Am Heart J* 1998;**136**:824–30.
12 **Trikas A**, Rallidis L, Hawkins P, *et al*. Comparison of usefulness between exercise capacity and echocardiographic indexes of left ventricular function in cardiac amyloidosis. *Am J Cardiol* 1999;**84**:1049–54.
13 **Schiller NB**, Shan PM, Crawford M, *et al*. Recommendation for quantification of the left ventricle by two-dimensional echocardiography. *J Am Soc Echocardiogr* 1989;**2**:358–67.
14 **Appleton CP**, Hatle LK, Popp RL. Demonstration of restrictive ventricular physiology by Doppler echocardiography. *J Am Coll Cardiol* 1988;**11**:757–68.
15 **Siegel RJ**, Roberts WC. Electrocardiographic observations in severe aortic valve stenosis: correlative necropsy study to clinical, hemodynamic, and ECG variables demonstrating relation of 12-lead QRS amplitude to peak systolic transaortic pressure gradient. *Am Heart J* 1982;**103**:210–21.
16 **Cerqueira MD**, Weissman NJ, Dilsizian V, *et al*. Standardized myocardial segmentation and nomenclature for tomographic imaging of the heart: a statement for healthcare professionals from the Cardiac Imaging Committee of the Council on Clinical Cardiology of the American Heart Association. *Circulation* 2002;**105**:539–42.
17 **Crotty TB**, Li C-Y, Edwards WD, *et al*. Amyloidosis and endomyocardial biopsy: correlation of extent and pattern of deposition with amyloid immunophenotype in 100 cases. *Cardiovasc Pathol* 1995;**4**:39–42.
18 **Wesbey GE**, Higgins CB, McNamara MT, *et al*. Effect of gadolinium-DTPA on the magnetic relaxation times of normal and infarcted myocardium. *Radiology* 1984;**153**:165–9.
19 **Kim RJ**, Judd RM. Gadolinium-enhanced magnetic resonance imaging in hypertrophic cardiomyopathy: in vivo imaging of the pathologic ubstrate for premature cardiac death? *J Am Coll Cardiol* 2003;**41**:1568–72.
20 **Mueller PS**, Edwards WD, Gertz MA. Symptomatic ischemic heart disease resulting from obstructive intramural coronary amyloidosis. *Am J Med* 2000;**109**:181–8.
21 **Maceira AM**, Joshi J, Prasad SK, *et al*. Cardiovascular magnetic resonance in cardiac amyloidosis. *Circulation* 2005;**111**:186–93.
22 **Smith TJ**, Kyle R, Lie JT. Clinical significance of histopathologic patterns of cardiac amyloidosis. *Mayo Clin Proc* 1984;**59**:547–55.
23 **Bergstrom J**, Gustavsson A, Hellman U, *et al*. Amyloid deposits in transthyretin-derived amyloidosis: cleaved transthyretin is associated with distinct amyloid morphology. *J Pathol* 2005;**206**:224–32.
24 **Metzler JP**, Fleckenstein JL, White CL 3rd, *et al*. MRI evaluation of amyloid myopathy. *Skeletal Radiol* 1992;**21**:463–5.
25 **Benson L**, Hemmingsson A, Ericsson A, *et al*. Magnetic resonance imaging in primary amyloidosis. *Acta Radiol* 1987;**28**:13–15.

IMAGES IN CARDIOLOGY

doi: 10.1136/hrt.2005.070110

Hypertrophic cardiomyopathy and left ventricular hypertrabeculation: evidence for an overlapping phenotype

Two female siblings (A and B) were referred for clinical screening following the sudden death of their mother aged 45 years from hypertrophic cardiomyopathy (diagnosed post-mortem). The sisters complained of fatigue, exertional dyspnoea (New York Heart Association functional class II), and infrequent palpitations. Their 12 lead ECGs are shown in panels A and B.

In patient A, the echocardiogram demonstrated asymmetric hypertrophy of the interventricular septum (maximum thickness 25 mm) with prominent trabeculations distally. In patient B there was very extensive hypertrabeculation in the mid and apical segments of the left ventricle with two myocardial layers visible in the parasternal short axis views (ratio of non-compacted to compacted layer 2.3). Their echocardiographic images are shown in panels C and D.

Left ventricular hypertrabeculation or left ventricular non-compaction (LVNC) is an increasingly recognised myocardial disorder characterised by excessive and prominent trabeculation of the left and/or right ventricle. Rare familial cases caused by mutations in cytoskeletal proteins (dystrobrevin, dystrophin), nuclear envelope proteins (emerin, lamin A/C), and tafazzin are described, but in the majority of adult patients with familial disease, the cause is unknown. In most adults with LVNC, the left ventricle is normal in size or dilated with impaired systolic function. Cases of hypertrophy are described in children, but we are unaware of any reports of adults within the same family with LVNC and hypertrophic cardiomyopathy. This family suggests that some cases of LVNC and hypertrophic cardiomyopathy may share a novel molecular mechanism related to disordered cardiac morphogenesis.

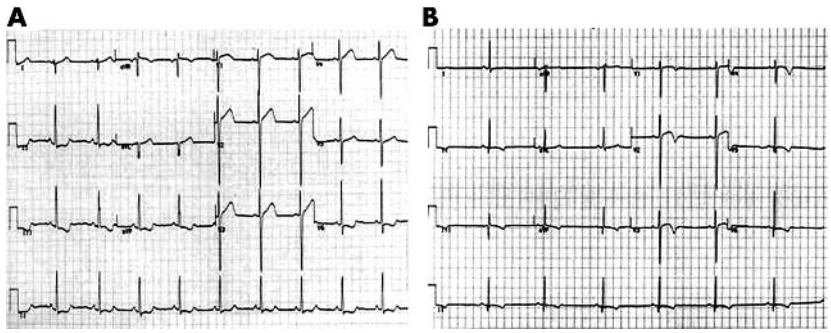

(A) The 12 ECG of sibling A shows right axis deviation with repolarisation abnormalities in inferior leads and V6 with deep S waves in leads V1–V3. (B) The ECG of sibling B shows normal axis with negative T waves in inferior and precordial leads.

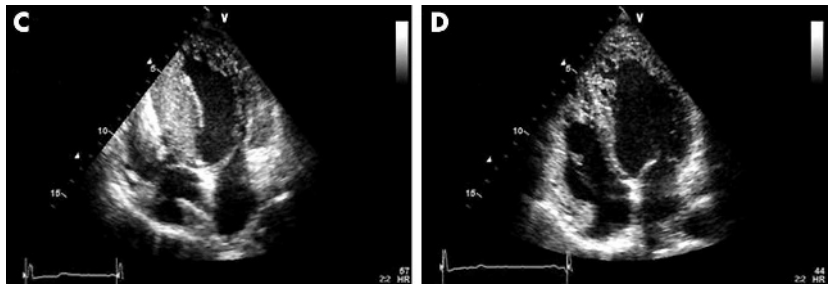

(C) Apical four chamber view of sibling A demonstrating asymmetric hypertrophy of the interventricular septum with prominent trabeculations distally. (D) The same view of the younger sister (sibling B) revealing prominent distal septal, and apical and free wall hypertrabeculation.

A A Pantazis
S K Kohli
P M Elliott
perry.elliott@uclh.nhs.uk